

# Structure and properties of transition fronts in accretion discs

Kristen Menou<sup>1,2</sup>, Jean-Marie Hameury<sup>3</sup> and Rudolf Stehle<sup>4</sup>

<sup>1</sup> *Harvard-Smithsonian Center for Astrophysics, 60 Garden Street, Cambridge, MA 02138, USA, kmenou@cfa.harvard.edu*

<sup>2</sup> *UPR 176 du CNRS, Département d’Astrophysique Relativiste et de Cosmologie, Observatoire de Paris, Section de Meudon, F-92195 Meudon Cédex, France*

<sup>3</sup> *UMR 7550 du CNRS, Observatoire de Strasbourg, 11 rue de l’Université, F-67000 Strasbourg, France, hameury@astro.u-strasbg.fr*

<sup>4</sup> *Astronomy Group, University of Leicester, Leicester LE1 7RH, U.K., rst@star.le.ac.uk*

12 April 2018

## ABSTRACT

We use high-resolution time-dependent numerical simulations of accretion discs around white dwarfs to study the structure and properties of transition fronts in the context of the thermal-viscous disc instability model. The thermal structure of cooling and heating fronts is dominated by radiative cooling and viscous heating, respectively, except in a very narrow precursor region in heating fronts where advection and radial transport of energy dominate. Cooling fronts are much broader than heating fronts, but the widths of both types of fronts scale with the local vertical scale height of the disc. We confirm that during a fair fraction of the propagation time of a cooling front, the structure of the inner disc is close to self-similar. The speed of heating fronts is  $\sim$  a few  $\text{km s}^{-1}$ , while the speed of cooling fronts is  $\sim$  a fraction of a  $\text{km s}^{-1}$ . We show that direct measurements of the speed of transition fronts probably cannot discriminate between various prescriptions proposed for the viscosity parameter  $\alpha$ . A natural prediction of the disc instability model is that fronts decelerate as they propagate in the disc, independent of the prescription for  $\alpha$ . Observation of this effect would confirm that dwarf nova outbursts are driven by the thermal-viscous instability. Most of our results also apply to low mass X-ray binaries in which the accreting object is a neutron star or a black hole.

**Key words:** accretion, accretion discs – instabilities – novae, cataclysmic variables – binaries : close

## 1 INTRODUCTION

It is widely accepted that the disk instability model (DIM) provides the correct description of dwarf nova outbursts (e.g Bath & Pringle 1982, Smak 1984, Lin, Papaloizou & Faulkner 1985, Cannizzo 1993a) and probably of soft X-ray transient events (van Paradijs & Verbunt 1984, Mineshige & Wheeler 1989, Cannizzo 1998a). In this model, the variability of a steadily fed thin accretion disc is due to the occurrence of a thermal-viscous instability in the disc. For a certain range of mass transfer rates from the secondary,  $\dot{M}_T$ , the effective temperature of a disc annulus lies within the unstable range 5000 – 8000 K, which corresponds to hydrogen recombination inside the disc. The unstable annulus then experiences a limit cycle during which matter is processed at rates larger or smaller than the mean rate  $\dot{M}_T$  (see Cannizzo 1993b or Osaki 1996 for reviews).

Transition fronts are essential to the DIM because they are the link between the local instability of an annulus and the global evolution of the disc. The time required by a

heating front to cross the disc is related (depending on wavelength) to the rise time of an outburst. Similarly, the time required for a cooling front to cross the disc defines the decay time of an outburst in the DIM (if the entire disc is brought to the hot state, the decay time is increased by a “viscous plateau” phase, see Cannizzo 1993a). Observations of the rise, decay and recurrence times therefore allow a direct test of the predictions of the DIM.

Several attempts to determine the structure and properties of transition fronts exist in the literature. Analytical studies lead only to qualitative results or to complex results that require numerical simulations for calibration (Meyer 1984, Lin et al. 1985, Vishniac & Wheeler 1996, Vishniac 1997). On the other hand, numerical studies have difficulties in correctly handling transition fronts because the fronts are very narrow and their propagation involves time and length scales which vary by several orders of magnitude in a single outburst. As discussed by Hameury et al. (1998, hereafter HMDLH), heating fronts are unresolved in most numerical

simulations while cooling fronts are often barely resolved, in particular close to the disc inner edge (see e.g. Cannizzo, Chen & Livio 1995). The poor resolution of transition fronts not only affects localized regions of the disc but it has also consequences for the global evolution of the disc (Cannizzo 1993a, HMDLH).

HMDLH have recently developed an implicit time-dependent numerical code which solves the disc equations on an adaptive grid. The code allows the resolution of very narrow structures in the disc at a relatively low computational cost. Here we use this code to study the detailed structure and the propagation velocities of heating and cooling fronts. We show that the width of any transition front is proportional to the disc pressure scale height  $H$ , and not to  $(HR)^{1/2}$  as proposed by Cannizzo et al. (1995). We confirm the existence of a self-similar regime of the hot inner disc during the propagation of a cooling front, and we discuss the possible reflections of cooling (resp. heating) fronts into heating (resp. cooling) fronts.

## 2 DISC INSTABILITY MODEL AND TRANSITION FRONTS

### 2.1 Disc equations

The time evolution of an accretion disc is driven by thermal-viscous processes. For a Keplerian disc the viscous equation, describing mass and angular momentum conservation, can be written as (Lightman, 1974; Pringle, 1981):

$$\frac{\partial \Sigma}{\partial t} = \frac{3}{R} \frac{\partial}{\partial R} \left[ R^{1/2} \frac{\partial}{\partial R} (\nu \Sigma R^{1/2}) \right], \quad (1)$$

where  $\nu$  is the kinematic viscosity,  $\Sigma$  is the surface density of the disc, and  $R$  is the distance from the central object. The viscosity is parameterized according to  $\nu = \alpha c_s H$ , where  $c_s$  is the sound speed in the disc midplane,  $H$  is the vertical scale height of the disc and the parameter  $\alpha$  ( $\leq 1$ ) describes our ignorance of the viscous processes. Shakura and Sunyaev (1973) first proposed this prescription with  $\alpha$  constant, but it was later shown by Smak (1984) that  $\alpha$  must be larger for the hot ionized disc than for the cold neutral disc in order to obtain large amplitude outbursts in the DIM.

In the following, we use two parameterizations often adopted in the literature. First, we adopt an  $\alpha_{\text{hot}} - \alpha_{\text{cold}}$  prescription and an arbitrary functional dependence of  $\alpha$  with the disc central temperature  $T_c$  which is similar to that used in HMDLH, i.e.

$$\log(\alpha) = \log(\alpha_{\text{cold}}) + [\log(\alpha_{\text{hot}}) - \log(\alpha_{\text{cold}})] \times \left[ 1 + \left( \frac{2.5 \times 10^4 \text{ K}}{T_c} \right)^8 \right]^{-1}, \quad (2)$$

where  $\alpha_{\text{hot}}$  and  $\alpha_{\text{cold}}$  are the two constant values of  $\alpha$  on the hot and the cold stable branches of the thermal equilibrium curves (or S-curves), respectively.

The second parameterization we consider is

$$\alpha = \alpha_0 (H/R)^{1.5}, \quad (3)$$

where  $\alpha_0$  is a constant ( $\alpha_0 = 50$  here). Such a dependence has been strongly advocated by several authors to explain the observed exponential decays of soft X-ray transients (Cannizzo, Chen & Livio, 1995; Vishniac & Wheeler,

1996). This interpretation may face some difficulties, however (§4.6). Note that the viscosity parameter  $\alpha \propto R^{3/4}$  in this case (e.g. Mineshige & Wheeler 1989).

The importance of allowing the disc outer edge,  $R_{\text{out}}$ , to vary with time in order to reproduce correct outburst cycles was emphasized by HMDLH and before by Smak (1984) and Ichikawa and Osaki (1992). Transition fronts are, however, localized structures and should not be influenced by the physical conditions at the disc outer edge. This is confirmed by a comparison between models differing only in whether or not  $R_{\text{out}}$  varies with time, which shows that the structure and the properties of the fronts are identical in the two classes of models (except when a front reaches  $R_{\text{out}}$ ). In the following, we assume that  $R_{\text{out}}$  is fixed.

The thermal equation (describing energy conservation; Faulkner, Lin & Papaloizou 1983, HMDLH) is given by:

$$\frac{\partial T_c}{\partial t} = \frac{2(Q^+ - Q^- + J)}{C_P \Sigma} - \frac{\Re T_c}{\mu C_P R} \frac{1}{R} \frac{\partial (R V_r)}{\partial R} - V_r \frac{\partial T_c}{\partial R}, \quad (4)$$

where  $Q^+$  and  $Q^-$  are the vertically-averaged rates of viscous heating and radiative cooling, respectively,  $\Re$  is the perfect gas constant,  $C_P$  is the specific heat at constant pressure of the gas,  $\mu$  its mean molecular weight and  $V_r$  its radial velocity (positive outward). The second term on the r.h.s. of Eq. (4) represents the contribution from pressure work and will be referred to as  $Q_{\text{pdv}}$ . The third term ( $Q_{\text{adv}}$ ) represents the contribution from energy advection. The term  $J$  (or equivalently  $Q_j$ ) accounts for the radial transport of energy (viscous or radiative). The (viscous) flux carried by turbulent eddies with a characteristic velocity  $v_e$  and size  $l_e$  is obtained dimensionally in the framework of the  $\alpha$ -prescription:

$$F_e = C_P \Sigma v_e \frac{\partial T_c}{\partial R} l_e = \frac{3}{2} \nu C_P \Sigma \frac{\partial T_c}{\partial R}, \quad (5)$$

and  $J$  is then given by:

$$J = \frac{1}{R} \frac{\partial}{\partial R} (R F_e). \quad (6)$$

A similar expression is obtained for the radiative transport of energy (Lin et al., 1985). Other prescriptions were proposed for  $J$  but they give results which are similar, in terms of outburst cycles, to those obtained with Eqs. (5) and (6) (HMDLH; see also §6).

Simulations show that most of the disc remains close to thermal equilibrium during its time evolution. In that case, the thermal equation basically reduces to  $Q^+ = Q^-$ . Transition fronts correspond, however, to regions far from thermal equilibrium in which the other terms in Eq. (4) are no longer negligible.

### 2.2 Numerical models

We use the numerical code developed by HMDLH with 800 grid points. This corresponds to about 100 points in the transition fronts, and is more than sufficient to avoid resolution-limited results.

All the models predict strictly periodic sequences of outbursts with (eventually) various amplitudes (see e.g. Fig. 8 of HMDLH). The sequences differ from one model to another (in number and amplitude of the outbursts). In the following, we refer to such a sequence as the outburst cycle of a model.

The disc outer radius is fixed to  $R_{\text{out}} = 4 \times 10^{10}$  cm. The disc inner radius,  $R_{\text{in}} = 5 \times 10^8$  cm, is equal to the white dwarf radius of mass  $M_1 = 1.2 M_{\odot}$ . A comparison of models with various mass transfer rates ( $\dot{M}_T$ ) shows that, although the outburst cycles differ from one model to another, the intrinsic structure and properties of transition fronts do not depend on  $\dot{M}_T$ . A value  $\dot{M}_T = 10^{-9} M_{\odot} \text{ yr}^{-1} = 6.66 \times 10^{16} \text{ g s}^{-1}$  is used in all models presented here.

We have considered four models to investigate the influence of the viscosity prescription on the structure and the properties of transition fronts. In three of them, we use an  $\alpha_{\text{hot}} - \alpha_{\text{cold}}$  prescription:  $\alpha_{\text{hot}} = 0.1$  and  $\alpha_{\text{cold}} = 0.02$  (model *h0.1.c0.02*),  $\alpha_{\text{hot}} = 0.2$  and  $\alpha_{\text{cold}} = 0.02$  (model *h0.2.c0.02*) and finally  $\alpha_{\text{hot}} = 0.1$  and  $\alpha_{\text{cold}} = 0.01$  (model *h0.1.c0.01*). The fourth model uses  $\alpha = 50(H/R)^{1.5}$  (model *50hr1.5*).

Global stability considerations (e.g. Cannizzo 1993b) and numerical simulations show that cooling fronts invariably appear in the outer disc. On the contrary, outbursts may be triggered anywhere in the disc, and both inside-out and outside-in heating fronts are observed in simulations (Smak 1984, HMDLH). All outbursts are of the inside-out type in the models presented here, except the largest amplitude outbursts of model *h0.1.c0.01* and all the outburst of model *50hr1.5* which are of the outside-in type.

### 2.3 Transition fronts

We define the location of a front,  $R_{\text{front}}$ , as the radius at which the central temperature  $T_c = 1.8 \times 10^4$  K in the disc. This value of  $T_c$  is a signature of the presence of a transition front because it lies in the range of central temperatures for which an annulus is thermally and viscously unstable. The speed of a front,  $V_{\text{front}}$ , is obtained by numerical differentiation of  $R_{\text{front}}$ .

In the following, the structure of transition fronts is shown each time for a specific value of  $R_{\text{front}}$ . Simulations show that the structures of transition fronts are qualitatively independent of their location in the disc. (In addition, cooling fronts evolve in a nearly self-similar way.) The general properties of the fronts do not depend on the viscosity prescription either.

From now on, the various terms  $Q/Q^+$  in Eq. (4) used to describe the thermal structure of a transition front are defined as positive if they correspond to a local heating and negative if they correspond to a local cooling in the disc (i.e. contrary to the positive convention for  $Q^-$  in Eq. (4)).

## 3 HEATING FRONTS

### 3.1 Structure of inside-out heating fronts

Figure 1 shows the structure of an inside-out heating front located at  $R_{\text{front}} \sim 3 \times 10^9$  cm in model *h0.1.c0.02*. It is characterized by a strong outflow of gas which is coincident with a sharp spike in the  $\Sigma$  profile and a steep gradient of  $T_c$  (or equivalently viscosity). The outflow and the formation of the spike in  $\Sigma$  were explained by Lin et al. (1985); they appear because the gas which carries excess angular momentum from the inner disc reaches colder regions where transport of angular momentum is reduced.

The dominant term in the thermal equation inside an

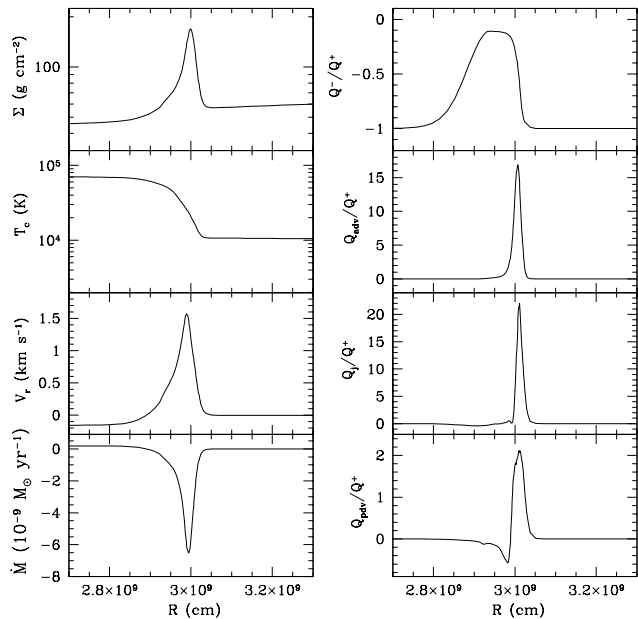


**Figure 1.** Structure of an inside-out heating front located at  $R_{\text{front}} \sim 3 \times 10^9$  cm (model *h0.1.c0.02*). The structure is dominated by a strong outflow of gas and by viscous heating, except in a narrow precursor region where radial diffusion and advection of energy dominate.

inside-out heating front is, by far, the viscous heating term  $Q^+$ . Figure 1 shows, however, the existence of a substructure in the front: a precursor region (narrower than the front itself) in which the energetics of the gas is dominated by advection and radial transport of energy. The contribution from pressure work is small but not negligible in the precursor region. The thermal structure of the front can be understood as follows. The hot gas which penetrates in colder regions of the disc carries a substantial amount of heat ( $Q_{\text{adv}}$ ). The gas is slowed down where the transport of angular momentum is reduced and it contracts ( $Q_{\text{pdv}}$ ). The precursor region is the region of strongest gradient of  $T_c$  (hence the large value of  $Q_j$ ).

Note that the region where heating ( $Q^+$ ) dominates over cooling is broader than the spike in  $\Sigma$  and the precursor region corresponds to the rising part of the spike of  $\Sigma$ .

### 3.2 Structure of outside-in heating fronts

Figure 2 shows the structure of an outside-in heating front located at  $R_{\text{front}} \sim 1.5 \times 10^9$  cm in model *50hr1.5*. The structure is expected to be different from that of an inside-out heating front since the matter crossing the transition region no longer carries excess angular momentum from the inner disc. Instead, this matter now corresponds to the bulk of accretion in the disc, while excess angular momentum is being freely carried away outward (Lin et al., 1985).

The accretion of hot gas is revealed by the strong inflow and the spike of  $\Sigma$  where the gas enters colder regions. Note the very steep gradient of  $T_c$  at the interface between the hot and cold regions of the disc and the presence of a

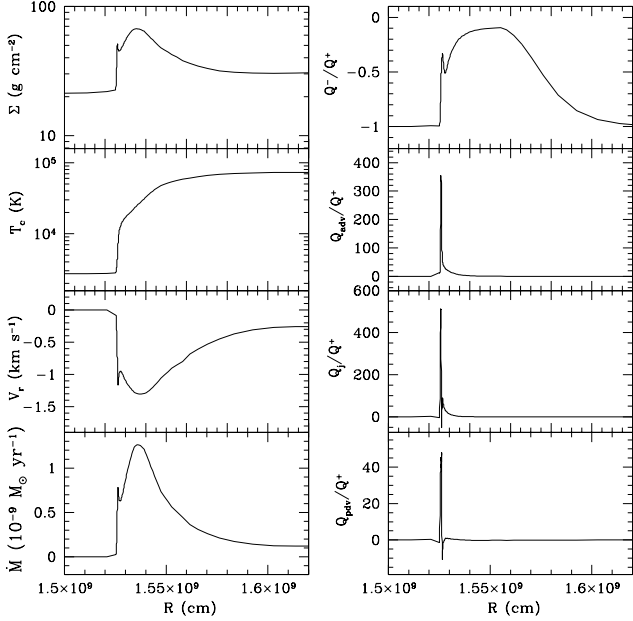


**Figure 2.** Structure of an outside-in heating front located at  $R_{\text{front}} \sim 1.53 \times 10^9$  cm (model *50hr1.5*). The structure is dominated by a strong inflow of gas and by viscous heating, except in a very narrow precursor region where radial diffusion and advection of heat dominate.

substructure in the profiles of  $\Sigma$ ,  $V_r$  and  $\dot{M}$  (corresponding to the precursor region).

The thermal structure of an outside-in heating front is similar to that of an inside-out heating front, despite their opposite direction of propagation. Viscous heating ( $Q^+$ ) is dominant, except in the precursor region where advection and radial diffusion of energy dominate the energetics of the gas. Once again, the pressure work term ( $Q_{\text{pdv}}$ ) is small but not negligible in the precursor region. The precursor region is, however, much narrower (as compared to the total width of the front) and its structure more complex than in an inside-out heating front.

### 3.3 Heating front velocity

Figure 3 shows the speed of heating fronts for the four models with various  $\alpha$ -prescriptions. Each dot represents the speed of the front,  $V_{\text{front}}$ , at a specific location  $R_{\text{front}}$  in the disc. Successive outbursts are triggered at nearly the same “ignition” radius during an outburst cycle in all the models, except in model *h0.1.c0.01* for which the outburst cycle is made of one outside-in (not shown here for clarity) and several inside-out outbursts. The simulations show that the front velocities strongly depend on the surface density profile at the onset of the thermal-viscous instability. Since mass piles up and diffuses from the outer regions of the disc during an outburst cycle, the front velocities vary from one outburst to another during the cycle, as seen from Fig. 3. For comparison, the sound speed is  $\sim 15$  km s $^{-1}$  for the characteristic temperature  $T_c = 18,000$  K in the transition front.

The velocity profiles of outside-in heating fronts (model

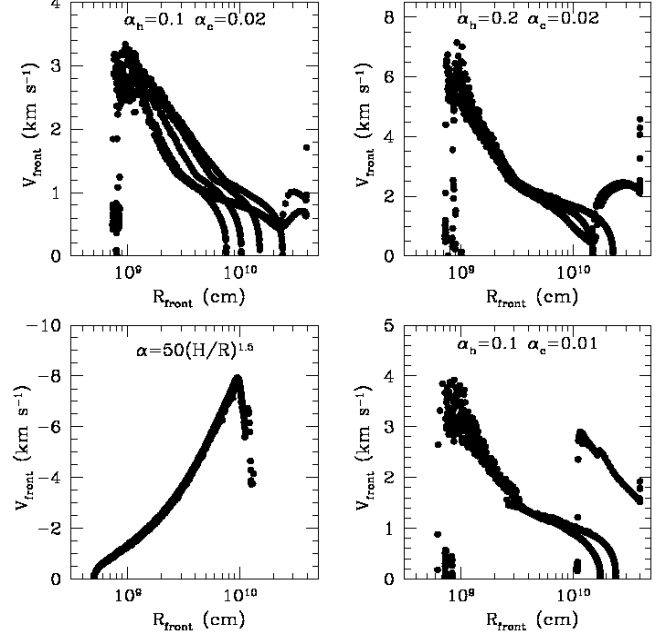


**Figure 3.** The four panels show the speed of successive heating fronts in our four models with various  $\alpha$ -prescriptions (dots). Outside-in (model *50hr1.5*) and inside-out (three other models) heating fronts slow down during their propagation in the disc. The speed of heating fronts significantly depends on the value of  $\alpha_{\text{hot}}$ .

*50hr1.5*) are very different from those of inside-out heating fronts (three other models). (This is not just due to the different  $\alpha$ -prescriptions.) A common characteristic of the two types of fronts is, however, a deceleration as the front propagates in the disc (a characteristic of cooling fronts as well; see §4.2).

It is not possible to compare quantitatively the speed of inside-out and outside-in heating fronts from Fig. 3 because a different  $\alpha$ -prescription is used in the models where the two types of fronts appear. Fortunately, we obtain both outside-in and inside-out outbursts in our model *h0.1.c0.01*. The maximum speeds of the two types of fronts in this model are similar ( $\sim 3$  km s $^{-1}$ ) but outside-in heating fronts cross the disc faster than inside-out heating fronts because their speed is high over a larger range of radii. This is in agreement with the fact that outside-in outbursts are known to produce more asymmetric lightcurves (i.e. shorter rise times) than inside-out outbursts (e.g. Smak 1984, HMDLH).

The speed of heating fronts slightly increases when  $\alpha_{\text{cold}}$  decreases. Increasing the value of  $\alpha_{\text{hot}}$  results in a substantial, approximately linear, increase of  $V_{\text{front}}$  which is of order of  $\alpha_{\text{hot}} c_s$  as in an ignition front (Meyer 1984). We find no significant change in the speed of heating fronts at a given  $R_{\text{front}}$  when the mass of the central white dwarf is decreased from  $M_1 = 1.2 M_\odot$  to  $0.6 M_\odot$  in model *h0.1.c0.02*.

It was argued by Lin et al. (1985) that the velocity of a transition front must be close to the speed of gas in the front. We compared the speed of heating fronts with the maximum speed of gas inside the fronts,  $V_{r,\text{max}}$  (see Figs. 1 and 2). The velocity of inside-out and outside-in heating fronts appears, indeed, close to  $V_{r,\text{max}}$  in the fronts. For instance,  $V_{\text{front}} \sim$

$3/2 V_{r,\max}$  in models *h0.1.c0.02* and *50hr1.5*. Note that the speed of the cold gas into which a heating front penetrates is negligibly small compared to the speed of the front.

### 3.4 Width of heating fronts

The width of a transition front was defined in HMDLH as the region of the disc over which the variation of the viscosity parameter  $\alpha = \alpha(T_c)$  is 90 % of the total variation between  $\alpha_{\text{cold}}$  and  $\alpha_{\text{hot}}$ . This definition, although appropriate for an  $\alpha_{\text{hot}} - \alpha_{\text{cold}}$  prescription, cannot be used when  $\alpha$  is a smooth function of  $H/R$  (in particular model *50hr1.5*).

We instead define the transition region as a zone with large thermal imbalance where the temperature changes on short timescales. More specifically, if the local timescale of change in temperature is

$$t_{\text{T}}(R) \equiv \left| \frac{\partial \ln T_c}{\partial t}(R) \right|^{-1}, \quad (7)$$

we define the transition region as the region of the disc where  $t_{\text{T}}(R) < 3t_{\text{T}}(R_{\text{front}})$ .  $R_{\text{front}}$  is the location of the front, as defined previously ( $T_c(R_{\text{front}}) \equiv 18,000$  K). The factor 3 is arbitrary but it has been chosen to give results close to what an eye estimate would give. We confirmed that the above definition leads to widths which are comparable to those found in HMDLH but also comparable to those found with a definition of the transition region based on a deviation of the ratio  $|Q^-/Q^+|$  from unity. (This last definition should be equivalent to the definition used by, e.g., Cannizzo 1994; Cannizzo et al. 1995.)

Figure 4 shows the fractional width ( $\delta w/R_{\text{front}}$ ) of heating and cooling fronts (dots) as a function of the front location in the four models with various  $\alpha$ -prescriptions. In each panel, the upper line of dots corresponds to cooling fronts and the lower line of dots corresponds to heating fronts. The width of cooling fronts is further discussed in §4.3.

The width of a heating front is roughly proportional to the local vertical scale height  $H$  (note that  $H = c_s/\Omega_K$  is defined at a fixed value  $T_c = 1.8 \times 10^4$  K here). This is not unexpected since, except for the narrow precursor region, the thermal structure of the front is dominated by the heating term,  $Q^+$ . Consequently, assuming that  $V_{\text{front}}$  varies much less rapidly than  $R_{\text{front}}^{3/2}$  (in agreement with our results, §3.3),  $\delta w$  is the distance traveled by the heating front in a few thermal timescales  $\tau_{\text{th}} \equiv (\alpha\Omega_K)^{-1}$  (e.g. Frank, King & Raine 1992), i.e.

$$\delta w \propto V_{\text{front}} \tau_{\text{th}} \propto (\alpha c_s / \alpha \Omega_K) \propto H \propto R_{\text{front}}^{3/2}. \quad (8)$$

These results are consistent with the conclusions of Meyer (1984, 1986) and Papaloizou & Pringle (1985).

A comparison of the various panels in Fig. 4 shows the influence of  $\alpha$  on the width of a heating front. Increasing  $\alpha_{\text{hot}}$  or decreasing  $\alpha_{\text{cold}}$  results in narrower fronts. It is not possible to interpret this result simply from Eq. (8), however, because the speed of heating fronts is also affected in a non-trivial way by changes in the viscosity parameter  $\alpha$  (cf §3.3).

In model *50hr1.5*, transition fronts have profiles of  $\delta w/R_{\text{front}}$  which are slightly flatter than the solid line ( $H/R_{\text{front}}$ ). According to the three other models, reduced widths are expected for larger values of  $\alpha_{\text{hot}}$ . The flatter profiles of  $\delta w$  are therefore consistent, at least qualitatively,

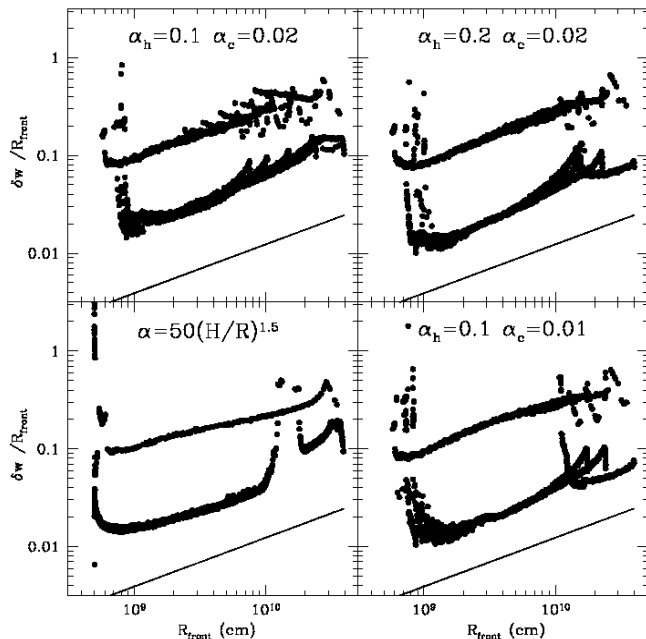


**Figure 4.** The four panels show the fractional width ( $\delta w/R_{\text{front}}$ ) of cooling fronts and heating fronts in our four models with various  $\alpha$ -prescriptions (dots). In each panel, the upper line of dots corresponds to the width of successive cooling fronts and the lower line of dots corresponds to the width of successive heating fronts. The solid line shows the fractional scale height of the disc ( $H/R_{\text{front}}$ ). Note that heating fronts in model *50hr1.5* are of the outside-in type.

with the additional variation of  $\alpha$  with radius in this particular model ( $\alpha \propto R^{3/4}$ ).

We also investigated the effect of varying the mass of the central object on the width of transition fronts. We decreased  $M_1$  from  $1.2 M_{\odot}$  to  $0.6 M_{\odot}$  in model *h0.1.c0.02*, which results in a reduced vertical gravity and therefore an increased vertical scale height  $H$  of the disc. At a given  $R_{\text{front}}$ , the front widths are increased, but the ratio of heating front (or equivalently cooling front) width to  $H$  is reasonably constant. This is additional evidence for a proportionality between  $\delta w$  and the local thermal timescale in the disc, which depends on  $M_1$  via  $\Omega_K$ .

### 3.5 Pairs of heating fronts

When the thermal-viscosity instability is triggered at a given ignition radius, two heating fronts appear which propagate in opposite directions in the disc. Because the ignition radius is often close to one of the disc edges, one of the two fronts is actually short-lived (i.e. quickly reaches the disc edge). The other heating front is long lived, propagates over a large range of radii and determines the global evolution of the disc.

It is possible, however, to obtain models in which a pair of heating fronts appears somewhere in the middle of the disc. Figure 5 shows such a situation (model *50hr1.5*), where an inside-out and an outside heating fronts appear around  $R \sim 1.5 \times 10^{10}$  cm. In that case, the two fronts contribute significantly to the global evolution of the disc. We referred

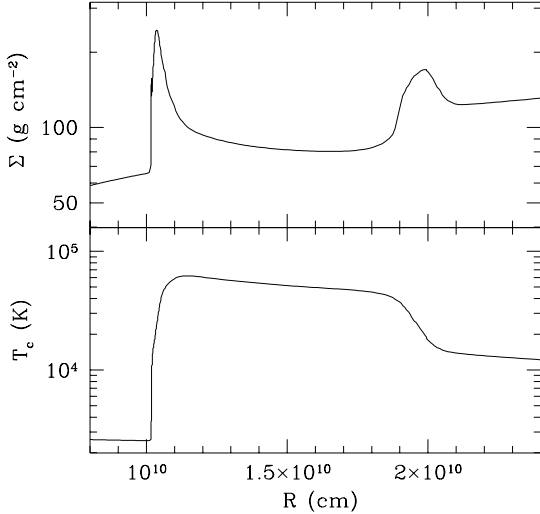


**Figure 5.** Radial profiles of  $\Sigma$  and  $T_c$  in a situation of coexistence of an inside-out and an outside-in heating front in the disc (model *50hr1.5*). Both fronts will significantly contribute to the global evolution of the disc.

to this type of intermediate outburst as an outside-in outburst.

More generally, simulations show that the value of the ignition radius in a specific model depends on the mass transfer accretion rate  $\dot{M}_T$  (HMDLH). This implies that a continuum of lightcurve shapes is possible, from quasi-symmetric (firm inside-out outburst) to strongly asymmetric (firm outside-in outburst). Consequently, the classification in two types of fronts initially proposed by Smak (1984) must be used with caution.

A careful look at Figure 3 of HMDLH reveals a sudden increase and then decrease of the inner accretion rate,  $\dot{M}_{acc}$ , which precedes the bulk of accretion in inside-out outbursts; this spike is very short lived, contains almost no energy, and is probably not observable. This is a signature of the arrival of an in-propagating heating front at the disc inner edge. This front is the short-lived companion of the long lived inside-out heating front which propagates over a large range of radii in the disc. Outside-in outbursts (e.g. Fig. 4 of HMDLH) do not show this burst of  $\dot{M}_{acc}$  because the outside-in heating front which reaches the disc inner edge is responsible for the bulk of the outburst accretion in that case.

### 3.6 Reflection of an inside-out heating front

The surface density after the passage of a heating front must be larger than the local value of  $\Sigma_{min}$  (the minimum density on the hot branch of the S-curve) to allow the front to propagate further in the disc. If not, a cooling front appears where  $\Sigma < \Sigma_{min}$  in the disc (just behind the  $\Sigma$  spike). Once the cooling front develops, the transport of excess angular momentum from the inner disc is strongly reduced and the

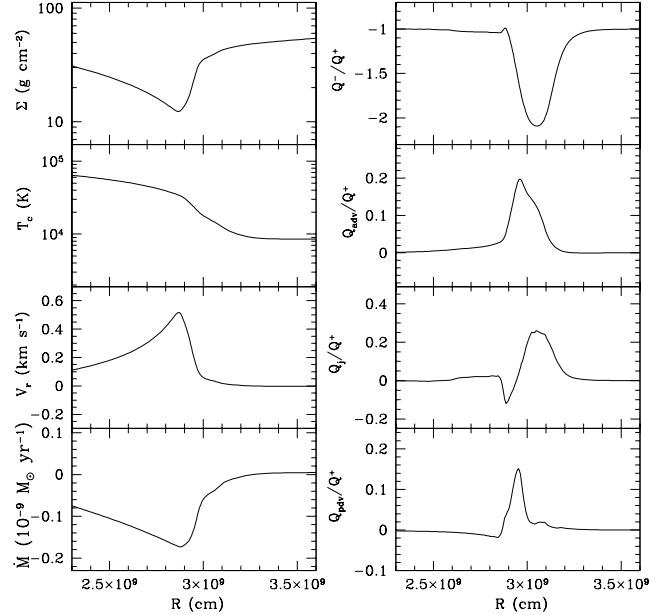


**Figure 6.** Structure of a cooling front located at  $R_{front} \sim 3 \times 10^9$  cm (model *h0.1.c0.02*). The structure is dominated by an outflow of gas and by radiative cooling.

propagation of the heating front is stopped. The spike in  $\Sigma$  then diffuses under the action of viscous processes. This process is usually referred to as a reflection, although it corresponds more exactly to the appearance of a new cooling.

In the case of outside-in fronts, matter flows from the outer parts of the disc, which contain most of the disc mass, so that  $\Sigma$  steadily increases at any given radius, and the heating front is always able to reach the disc inner edge without being reflected in our models.

The situation is quite different for inside-out heating fronts, for which mass is transferred from the inner parts to the outer parts of the disc. The comparatively small amount of mass in the inner disc leads to several reflections of inside-out heating fronts during one outburst cycle. After these multiple reflections, an inside-out heating front can reach  $R_{out}$  without being reflected because enough mass has accumulated in the outer disc and  $\Sigma$  behind the front remains above  $\Sigma_{min}$  during the entire propagation.

The reflections also occur in mini-outbursts (as compared to “normal” outbursts in which most of the disc – if not all – undergo a transition to the hot state) which are found in many numerical models (see e.g. Cannizzo 1993a, HMDLH). The significance of these mini-outbursts is unclear because they have probably not been observed.

## 4 COOLING FRONTS

### 4.1 Structure of cooling fronts

Figure 6 shows the structure of a cooling front located at  $R_{front} \sim 3 \times 10^9$  cm in model *h0.1.c0.02*. The innermost, hot, regions of the disc accrete at a much higher rate than the outer cold regions (see e.g. Fig. 9 of Cannizzo et al. 1995).

A substantial amount of angular momentum flows outward in the inner regions of the disc. The gas which carries this excess angular momentum is stopped when it reaches colder regions of the disc, where the transport of angular momentum is reduced. This results in a large outflow and an abrupt increase of  $\Sigma$  where rapid cooling sets in, as seen from Fig. 6.

As noted by Vishniac & Wheeler (1996) (see also Vishniac 1997), the inner disc is in quasi-steady state during the propagation of a cooling front; the accretion rate is almost independent of radius and it slowly decreases with time. The profiles of  $\Sigma$  and  $T_c$  in these regions (not shown in Fig. 6, but see, e.g., Fig. 5a of HMDLH) are close to those of the steady solution of Shakura & Sunyaev (1973). Between the inner quasi-steady disc and the front itself, there is a relatively broad region (called precursor region by Vishniac & Wheeler 1996) where the profiles of  $\Sigma$  and  $T_c$  deviate substantially from the Shakura-Sunyaev profiles.

Figure 6 shows that the thermal structure of a cooling front is dominated, although not strongly, by radiative cooling ( $Q^-$ ): in first approximation, gas freely cools inside a cooling front (Vishniac & Wheeler 1996). The three non-local terms in the energy equation, namely  $Q_{\text{adv}}$ ,  $Q_j$  and  $Q_{\text{pdv}}$ , are small but not negligible. The radial transport of energy ( $Q_j$ ) occurs in the region of strong gradient of  $T_c$ . Advection of energy and adiabatic compression of the gas occur mainly in a region corresponding to the outflow of gas, i.e. where the gas which carries a substantial amount of heat ( $Q_{\text{adv}}$ ) is compressed as it enters colder regions of the disc ( $Q_{\text{pdv}}$ ).

## 4.2 Cooling front velocity

Figure 7 shows the speed of cooling fronts in the four models with various  $\alpha$ -prescriptions. Successive cooling fronts in an outburst cycle appear at various locations in the disc in models using an  $\alpha_{\text{hot}} - \alpha_{\text{cold}}$  prescription. All the cooling fronts appear at the same location, close to the disc's outer edge, in model *50hr1.5*. The initial speed of all cooling fronts is relatively high but soon, as they propagate inward, they relax to a reduced and common asymptotic speed which depends only on the current location of the front in the disc,  $R_{\text{front}}$ , in agreement with early calculations by Cannizzo (1994).

The effect of varying  $\alpha_{\text{cold}}$  on the (asymptotic) speed of a cooling front is small (at most). Increasing the value of  $\alpha_{\text{hot}}$  results, however, in higher asymptotic speeds.

In the asymptotic regime,  $V_{\text{front}}$  has a weak dependence on  $R_{\text{front}}$ . This is especially true in models with an  $\alpha_{\text{hot}} - \alpha_{\text{cold}}$  prescription (see also Cannizzo 1994). The different variation of  $V_{\text{front}}$  with  $R_{\text{front}}$  in model *50hr1.5* can be accounted for by the variation of  $\alpha$  with radius in this specific model, according to the scaling of  $V_{\text{front}}$  versus  $\alpha_{\text{hot}}$  in the three other models. Note that the sharp increase of  $V_{\text{front}}$  close to the disc inner edge observed in all models is a boundary condition effect: the surface density  $\Sigma$  goes to zero at  $R_{\text{in}}$  and this causes the front to propagate faster as  $\Sigma$  is closer to  $\Sigma_{\text{min}}$  in the innermost regions of the disc.

The speed of a cooling front, at a given radius  $R_{\text{front}}$ , is slightly sensitive to the mass of the central object. We obtained an increase of  $V_{\text{front}} \sim 30\%$  in the asymptotic regime when the mass  $M_1$  was changed from  $1.2 M_{\odot}$  to  $0.6 M_{\odot}$ .

$V_{\text{front}}$  in the asymptotic regime is not much larger than the speed of the hot gas into which the front penetrates; both

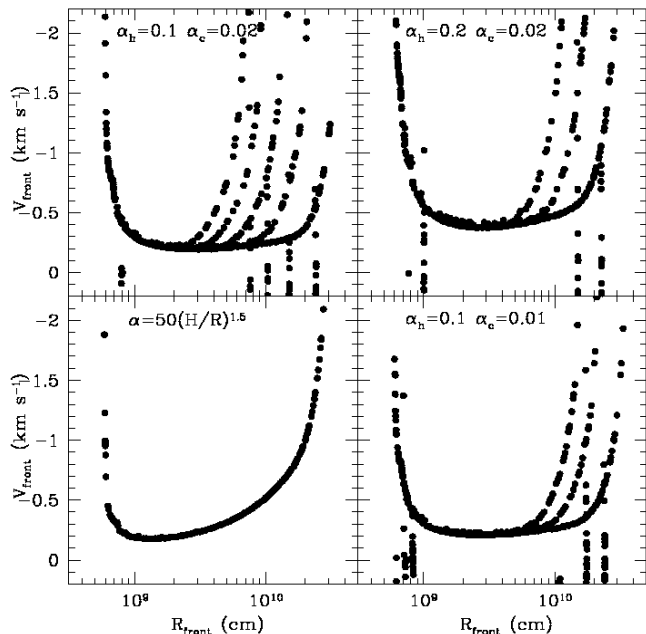


**Figure 7.** The four panels show the speed of successive cooling fronts in our four models with various  $\alpha$ -prescriptions (dots). Cooling fronts appearing at various radii in the outer disc quickly converge to the same asymptotic speed (in a given model) as they propagate inward. (Note that all cooling fronts appear at the same location in model *50hr1.5*.) The asymptotic speed of a cooling front slightly depends on the value of  $\alpha_{\text{hot}}$ .

are of order of a fraction of  $1 \text{ km s}^{-1}$ . This is consistent with the idea that an evolution of the inner hot disc on a viscous timescale is typically required to allow the propagation of the cooling front (Lin et al. 1985, Vishniac & Wheeler 1996). But contrary to the case of heating fronts, we find no good correlation between the value of  $V_{\text{r,max}}$  inside the transition region and the speed of cooling fronts.

Recently, Bobinger et al. (1997) directly determined the speed of a cooling front with the eclipse mapping technique. They observed the evolution of the brightness temperature profile in the disc of the dwarf nova IP Peg during four successive days of its decay from outburst. They infer a mean value of  $V_{\text{front}} \sim 0.8 \text{ km s}^{-1}$  over the four days, which is consistent with the speeds shown in Fig. 7. It will be difficult, however, to determine the viscosity parameter  $\alpha$  from such observations, even if variations of  $V_{\text{front}}$  with  $R_{\text{front}}$  were detected. For instance, models *h0.1.0c0.02* and *50hr1.5* produce very different outburst cycles which could be distinguished from observed lightcurves; yet the variation of  $V_{\text{front}}$  with  $R_{\text{front}}$  is not drastically different. A strong prediction of the DIM (which probably holds for any reasonable  $\alpha$ -prescription) is, however, the rapid decrease of  $V_{\text{front}}$  with  $R_{\text{front}}$  shortly after the appearance of a cooling front. The detection (or non-detection) of this characteristic would be strong evidence (or disproof) that the DIM – as we understand it – operates in accretion discs.

Vishniac & Wheeler (1996) proposed an analytical model of cooling fronts which uses the numerical results of Cannizzo et al. (1995) as calibration. In the derivation of Vishniac & Wheeler (1996), the speed of a cooling front

does not depend on the physical conditions in the cold gas behind the front. This is in agreement with the independence of  $V_{\text{front}}$  with  $\alpha_{\text{cold}}$  observed in our simulations.

Vishniac & Wheeler (1996) predict a speed for the cooling front

$$V_{\text{front}} = \alpha_{FCF} \left( \frac{H}{R} \right)^{0.54} \quad (9)$$

if  $\alpha = 50(H/R)^{1.5}$  (and assuming a Kramer's law opacity is valid for the hot gas), and a speed

$$V_{\text{front}} = \alpha_{\text{hot}CF} \left( \frac{H}{R} \right)^{7/10} \quad (10)$$

in the case of an  $\alpha_{\text{hot}} - \alpha_{\text{cold}}$  prescription. Here  $\alpha_F$  and  $c_F$  are the viscosity parameter and the sound speed at the cooling front (i.e. where rapid cooling sets in).

Equation (9) predicts a  $V_{\text{front}}$  which is slightly smaller (20% typically) than what we find in the asymptotic regime of model *50hr1.5* but the dependence with  $R_{\text{front}}$  appears good. Equation (10) predicts, however, a  $V_{\text{front}}$  which is typically twice as small as what is observed in the asymptotic regime of model *h0.1.c0.02*.

Vishniac & Wheeler (1996) assume that the gas velocity at the cooling front,  $V_F$ , is  $\sim 1/6 \alpha_{FCF}$  and that  $V_F$  is much larger than the cooling front velocity. In our simulations,  $V_F \sim 1/7 \alpha_{FCF}$ , but the cooling front velocity is not much smaller than  $V_F$ . The ratio of the gas velocity at the cooling front to the cooling front velocity is typically of order 2 (see Figs. 6 and 7). Neglecting  $V_{\text{front}}$  is probably one of the reason for the discrepancy between the predictions of Vishniac & Wheeler (1996) and our results.

### 4.3 Width of cooling fronts

Figure 4 shows the width of cooling fronts in the four models with various  $\alpha$ -prescriptions. Cooling fronts are much broader than heating fronts but their width  $\delta w$  remains proportional to  $H$ . As for heating fronts, we interpret the width of a cooling front as the distance traveled by the front during a few thermal timescales (the thermal structure of the front being dominated by radiative cooling):  $\delta w$  is proportional to  $R_{\text{front}}^{3/2} \propto H$  (Eq. (8)). \*

This conclusion is in contradiction with the results of Cannizzo et al. (1995) who find  $\delta w = \sqrt{HR}$  in a numerical model using  $\alpha = 50(H/R)^{1.5}$ . The profiles of  $\delta w/R_{\text{front}}$  as a function of  $R_{\text{front}}$  shown in Fig. 4 for model *50hr1.5* are

\* Naively, one would expect from Eq. (8) smaller  $\delta w$  for cooling fronts than for heating fronts (because of smaller  $V_{\text{front}}$ ). Equation (8) does not take into account, however, several complications in the problem. The thermal timescale  $\tau_{\text{th}} \equiv (\alpha\Omega_K)^{-1}$ , which is very different for annuli in the hot and the cold regions of the disc, is probably increased because of the ionization energy in transition regions (Papaloizou & Pringle 1985). The precursor region drives out of thermal equilibrium the disc annuli entering the transition region in the case of heating fronts (see Fig. 9), while there is no equivalent for cooling fronts. Finally, radiative cooling clearly does not dominate the thermal structure of a cooling front as much as viscous heating does in a heating front, which probably leads to comparatively longer thermal timescales for cooling fronts. A key feature that Eq. (8) includes, however, is the strong variation of the thermal timescale with radius.

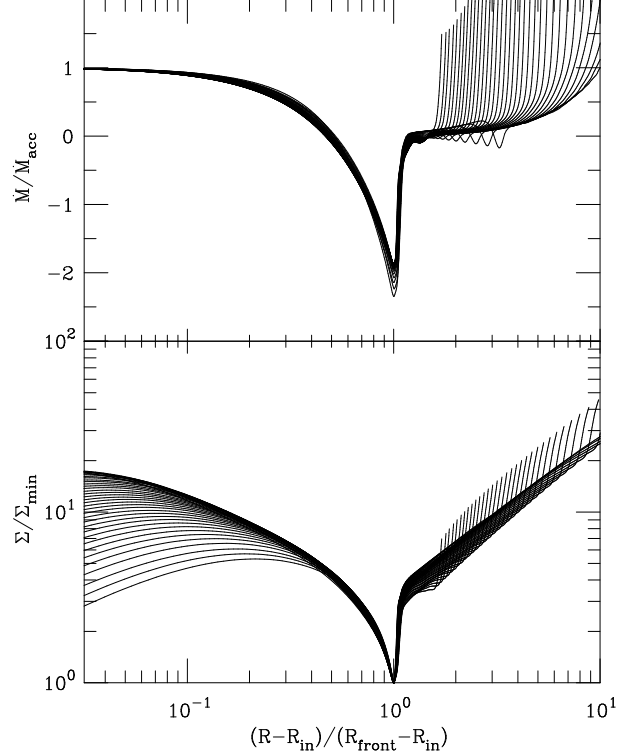


**Figure 8.** Successive normalized profiles of  $\Sigma$  and local mass flow rate  $\dot{M}$  as a function of the dimensionless radius  $(R - R_{\text{in}})/(R_{\text{front}} - R_{\text{in}})$  during the propagation of a cooling front (model *h0.1.c0.02*). The superposition of profiles reveals the nearly self-similar evolution of the inner hot disc.

consistent with those of Cannizzo et al. (1995). Cannizzo et al. (1995) claim that  $\delta w = \sqrt{HR}$  is also true in models using an  $\alpha_{\text{hot}} - \alpha_{\text{cold}}$  prescription. Our three models with  $\alpha_{\text{hot}} - \alpha_{\text{cold}}$  prescriptions rule out this possibility and show that  $\delta w \propto H$ . As mentioned previously, we interpret the flatter profiles of  $\delta w$  in model *50hr1.5* as due to the variation of  $\alpha$  with radius in this particular model. Models using  $\alpha = \alpha_0(H/R)^n$  with various  $n$  produce various slopes for the profiles of  $\delta w$  as a function of  $R_{\text{front}}$ .

A comparison of the various panels in Fig. 4 shows that the effect of varying  $\alpha$  on the width of a cooling front is small.

### 4.4 Self-similar solutions

Vishniac (1997) proposed a self-similar solution for the structure of the hot inner disc during the propagation of a cooling front. We confirm the existence of a self-similar regime, although the self-similarity described here is somewhat different from the solution of Vishniac (1997) because  $\Sigma$  is found to scale naturally with  $\Sigma_{\text{min}}$ . We leave a detailed analysis of the self-similar solution for a future paper, but we give here our main qualitative results.

Figure 8 shows successive profiles of  $\Sigma$  and local mass transfer rate  $\dot{M}$  during the propagation of a cooling front in model *h0.1.c0.02*, when the asymptotic regime is reached. The profiles of  $\Sigma$  have been normalized to the minimum surface density in the cooling front, which is extremely close

to  $\Sigma_{\min}$  at  $R_{\text{front}}$ . This is not unexpected, since the transition from the hot to the cold state occurs precisely when  $\Sigma$  reaches  $\Sigma_{\min}$ . The mass flow rate  $\dot{M}$  has been normalized, following Vishniac (1997), to the mass transfer rate at the disc inner edge,  $\dot{M}_{\text{acc}}$ . The horizontal coordinate chosen here is  $(R - R_{\text{in}})/(R_{\text{front}} - R_{\text{in}})$  in order to minimize the effect of the inner boundary condition on the profiles. The value of  $R_{\text{front}}$  varies by more than an order of magnitude for the successive profiles shown in Fig. 8 and yet the normalized  $\Sigma$  and  $\dot{M}$  remain remarkably similar: except for the effect of boundary conditions, the evolution of the inner hot disc is close to self-similar.

The mass accretion rate onto the compact object,  $\dot{M}_{\text{acc}}$ , is proportional to  $\dot{M}_{\text{front}}$  at the transition radius. But

$$\dot{M}_{\text{front}} = 2\pi R_{\text{front}} \Sigma(R_{\text{front}}) V_r(R_{\text{front}}), \quad (11)$$

$\Sigma(R_{\text{front}}) = \Sigma_{\min}(R_{\text{front}}) \propto R_{\text{front}}^{1.1}$  (e.g. HMDLH), and  $V_r(R_{\text{front}})$  is comparable to the front velocity. If  $\alpha$  in the hot inner disc is constant, one expects a weak dependence of  $V_r(R_{\text{front}})$  with  $R_{\text{front}}$  and  $\dot{M}_{\text{acc}} \propto R_{\text{front}}^n$ , with  $n$  slightly larger than 2. Indeed, numerical simulations show that  $n \simeq 2.2$  for an  $\alpha_{\text{hot}} - \alpha_{\text{cold}}$  prescription, and  $n \simeq 2.4$  when  $\alpha \propto (H/R)^{1.5}$ .

As discussed by Vishniac (1997), the hot inner disc evolves on a viscous time during the propagation of a cooling front, and is therefore very close to thermal equilibrium. The inner disc empties as a result of accretion onto the compact object, but also because an even larger amount of mass is transferred into the cold outer regions of the disc. These parts of the disc are essentially frozen on the time scale of propagation of the cooling front. Consequently,  $\Sigma(R)$  behind the front remains constant in time and is equal to  $K\Sigma_{\min}(R)$ , where  $K$  is a self-similarity constant that depends on the mass of the primary and the viscosity parameter  $\alpha$  both in the hot and the cold regions of the disc. For the parameters of Fig. 8,  $K \sim 4$ . The constant  $K$  increases with the mass of the primary (for example,  $K \sim 6 - 7$  for a  $7 M_{\odot}$  primary typical of a black hole SXT).

The sudden increase of  $\Sigma$  just after the passage of a cooling front is actually smaller in the pre-self-similar regime, so that  $\Sigma/\Sigma_{\min}$  increases as the front propagates toward the asymptotic regime. This accounts for the density profile in the outer disc which is relatively flat close to the outer edge, steepens at smaller radii and finally becomes proportional to  $\Sigma_{\min} \propto r^{1.1}$  in the self-similar regime.

#### 4.5 Reflection of a cooling front

The sudden increase of  $\Sigma$  just after the passage of a cooling front cannot be arbitrarily large (Vishniac, 1997). If  $\Sigma > \Sigma_{\max}$  behind the cooling front, an inside-out heating front develops and propagates over some distance in the disc because  $\Sigma$  is substantially larger than  $\Sigma_{\min}$  in the outer disc. The initial cooling front soon disappears as hot gas from the outer regions of the disc accretes inward.

This situation corresponds to the reflection of a cooling front into a heating front and it occurs whenever  $\Sigma_{\max}/\Sigma_{\min}$  is too small. The ratio  $\Sigma_{\max}/\Sigma_{\min}$  has a weak radial dependence ( $R^{0.02-0.03}$ ; e.g. HMDLH). If the self-similarity constant  $K$  is too large, the cooling front will experience a reflection typically when it enters the self-similar regime: the gradual increase of  $\Sigma/\Sigma_{\min}$  preceding the self-similar regime

will drive  $\Sigma$  behind the front above  $\Sigma_{\max}$  and lead to the reflection.

The multiple reflections of cooling fronts are well known if  $\alpha_{\text{cold}} = \alpha_{\text{hot}}$  (Smak, 1984). In this case, the inner disc can never be brought entirely into quiescence, and the reflected transition fronts propagate back and forth in a restricted region of the disc, causing small amplitude quasi-oscillations of the disc luminosity.

Note that because  $K$  increases with the mass of the primary, the reflections of cooling fronts are more likely to occur in BH SXTs than in neutron star SXTs or dwarf novae.

#### 4.6 Exponential decays

We reexamine, in light of our results on cooling fronts, the claim by Cannizzo et al. (1995; see also Vishniac & Wheeler 1996) that  $\alpha = \alpha_0(H/R)^{1.5}$  is necessary to account for exponential decays of soft X-ray transients (SXTs; but see also the similarity between SXTs and dwarf novae pointed out by Kuulkers, Howell & van Paradijs 1996)

Our simulations show that the inner accretion rate  $\dot{M}_{\text{acc}} \propto R_{\text{front}}^n$  in the self-similar regime of propagation of a cooling front ( $n = 2 - 2.5$  depending on the  $\alpha$ -prescription).

Since X-rays are produced close to the central object in an SXT, the exponentially decaying lightcurves imply an exponential decay of  $\dot{M}_{\text{acc}}$  as well, i.e.

$$\frac{d\dot{M}_{\text{acc}}}{dt} \propto \dot{M}_{\text{acc}}. \quad (12)$$

If we assume that the decay phase corresponds to the propagation of a cooling front in the disc and that our results apply (no irradiation effect is included in our calculations), then

$$\frac{d\dot{M}_{\text{acc}}}{dt} \propto R_{\text{front}}^{n-1} V_{\text{front}} \propto \dot{M}_{\text{acc}} \frac{V_{\text{front}}}{R_{\text{front}}}, \quad (13)$$

and an exponential decay is possible only if  $V_{\text{front}}/R_{\text{front}}$  remains constant, meaning that  $R_{\text{front}}$  must also vary exponentially with time:

$$V_{\text{front}} = \frac{dR_{\text{front}}}{dt} \propto R_{\text{front}}. \quad (14)$$

Note that this requirement was already deduced, although differently, by Cannizzo et al. (1995) and Vishniac & Wheeler (1996).

Figure 7 shows that  $V_{\text{front}}$  is primarily independent of  $R_{\text{front}}$  (in the asymptotic regime) in the three models with  $\alpha_{\text{hot}} - \alpha_{\text{cold}}$  prescriptions. On the contrary, model *50hr1.5* shows a variation of  $V_{\text{front}}$  with  $R_{\text{front}}$  which is linear in first approximation. Our calculations therefore confirm that a dependence of the viscosity parameter  $\alpha$  with radius (close to  $\alpha \propto R^{3/4}$  like in model *50hr1.5*) is required to obtain exponential decays of  $\dot{M}_{\text{acc}}$  in the DIM.

A major concern however is the relevance of interpreting exponentially decaying lightcurves as due to the propagation of a cooling front in the discs of SXTs. In particular, Shahbaz et al. (1998) argue that both linear and exponential decays are observed in SXTs (see also the compilation of lightcurves by Chen et al. 1997). Since there is no obvious physical reason why  $\alpha$  would vary markedly from one system to another, the possibility that both linear and exponential decays are observed in SXTs argues against an interpreta-

tion of the exponential decays as due to a specific functional form of  $\alpha$ .

An alternative and perhaps more promising explanation for the exponential decays has been proposed by King & Ritter (1998). The authors argue that strong irradiation of the disc may prolongate the phase during which the entire disc is in the hot state and lead to an evolution of the disc on a (long) viscous time (see however Dubus et al. 1998).

#### 4.7 Cooling fronts and the periodicity of outburst cycles

The asymptotic regime of cooling front propagation has a profound influence on the outburst cycles experienced by the disc. Since the inner hot disc evolves in a self-similar way, the profiles of  $\Sigma$  and  $T_c$  inside  $R_{\text{front}}$  are uniquely determined by the current value of  $R_{\text{front}}$ .

A cooling front following a heating front that reached the outermost regions of the disc therefore propagates in the exact same way a previous cooling front starting from  $R_{\text{out}}$  did. This type of cooling front erases the history of the disc and is responsible for the periodicity of the outburst cycles in the simulations. An outburst cycle ends and a new cycle begins when a heating front reaches  $R_{\text{out}}$  (also corresponding to the largest amplitude outbursts).

Observed outburst cycles in dwarf novae are usually regular but not periodic (e.g. Warner 1995, Cannizzo & Mattei 1992). This may hint that a piece of physics is missing in the standard DIM. A variation of the mass transfer accretion rate  $\dot{M}_T$  appears as a natural candidate for explaining the irregularity of observed cycles.

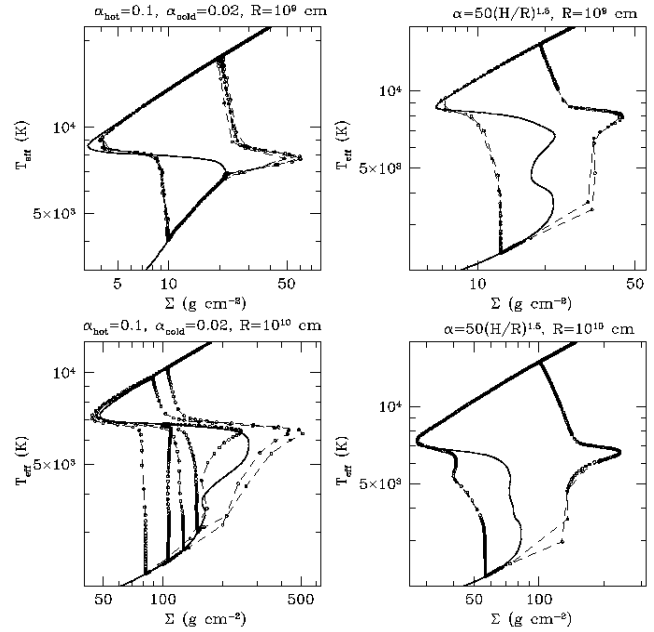
## 5 EVOLUTION AROUND S-CURVES

Figure 9 shows limit cycles experienced by two disc annuli in models *h0.1.c0.02* and *50hr1.5* in the  $\Sigma - T_{\text{eff}}$  plane, where  $T_{\text{eff}}$  is the effective temperature of the disc.

Global effects (i.e. influence by neighboring annuli) appear when an annulus no longer lies on the S-curve. The passage of a cooling front corresponds to a jump from the upper hot branch of the S-curve to the lower cold branch. Inversely, the passage of a heating front corresponds to the jump from the lower branch to the upper branch. Note that the maximum value of  $\Sigma$  reached by a disc annulus on the lower cold branch of the S-curve during a limit cycle is indicative of the proximity of this annulus to the ignition radius in the disc.

Figure 9 shows the evolution of disc annuli during the passage of a transition front: a sudden increase of  $\Sigma$  is as good a signature of the transition as a change of  $T_{\text{eff}}$  is. For a cooling front, the sudden change of  $\Sigma$  shortly precedes the phase of rapid cooling of the annulus. For a heating front, the sudden change of  $\Sigma$  corresponds to the passage of the spike of  $\Sigma$ . This shows that inside a transition front, the viscous time is not much larger but comparable to the thermal time since surface density and effective temperature vary on similar timescales.

The complexity of the limit cycles experienced by the annulus at  $R = 10^{10}$  cm in model *h0.1.c0.02* is due to the many reflections of inside-out heating fronts into cooling fronts around  $10^{10}$  cm in this model. Note that the



**Figure 9.** Limit cycles experienced by disc annuli located at  $R = 10^9$  and  $10^{10}$  cm in the  $\Sigma - T_{\text{eff}}$  plane. The left panels correspond to model *h0.1.c0.02* and the right ones to model *50hr1.5*. The solid lines are the thermal equilibrium curves, where  $Q^+ = Q^-$  (standard S-curves). The dashed lines trace the successive states of a disc annulus, while the density of circles is representative of the amount of time spent by an annulus in a given state. The evolution of the disc annulus shown in the lower left panel is complex because this annulus is located in a region of front reflections.

track followed by the annulus states during the successive jumps from the upper branch to the lower branch do not cover each other in that case because cooling fronts have not yet reached the asymptotic regime at  $10^{10}$  cm in model *h0.1.c0.02*.

Note that the evolutions around S-curves shown here differ significantly from the results of Ludwig, Meyer-Hofmeister & Ritter (1994) using the theory of infinitely thin transition fronts (Meyer 1984). Some additional limitations of the theory were pointed out by Ludwig & Meyer (1998).

## 6 VALIDITY OF THE DISC EQUATIONS FOR THE TRANSITION FRONTS

It is standard in the theory of thin accretion discs to assume that the vertical structure of the disc is decoupled from its radial structure because the former evolves on much shorter timescales than the latter (e.g. Frank et al. 1992). Because  $\Sigma$  and  $T_{\text{eff}}$  vary on similar timescales, this assumption is no longer valid inside transition fronts: the vertical structure is coupled to the radial structure of the disc. In particular, radial transport of energy becomes important in the transition regions, while the transport occurs only vertically in steady thin discs (Frank et al. 1992).

A correct treatment of the coupling between the radial and vertical structures of the disc would probably involve

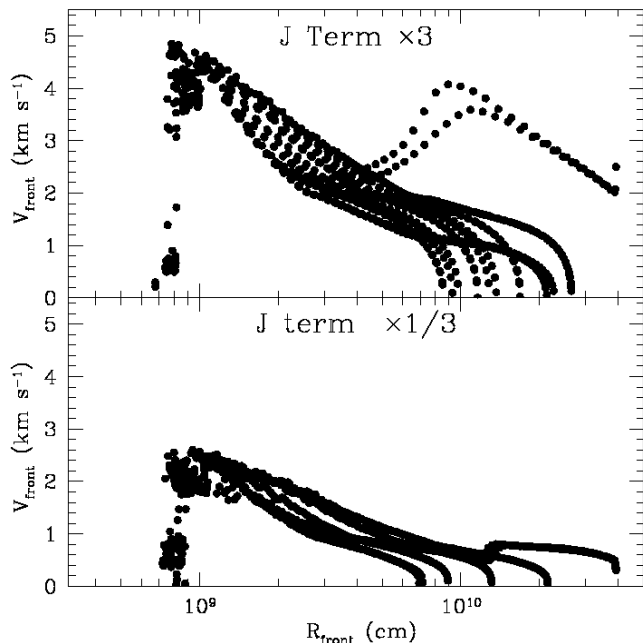


**Figure 10.** An illustration of the sensitivity of the propagation velocity of heating fronts to the poorly known efficiency of radial transport of energy (term  $J$  in Eq. (2)), in model *h0.1.c0.02*.

2D simulations. For simplicity, however, the radial transport of energy is usually parameterized in a simple manner in 1D disc equations (see also the approximations of decoupling used for the determination of the cooling rate  $Q^-$ , HMDLH). The fact that various prescriptions exist for  $J$  (Eq. (4)) shows that the radial transport of energy in the disc is not well known, and surely not within a factor of a few.

Figure 10 shows the effect on the speed of heating fronts of increasing or decreasing by a factor 3 the intensity of the term  $J$ . The large uncertainty in  $J$  translates into a significant uncertainty on the speed of heating fronts. (Note that the speed of cooling fronts is not affected because the radial transport of energy has a minor influence on their structure; cf Fig. 6).

An additional concern about the validity of the disc equations inside transition fronts comes from the narrowness of the fronts. Lin et al. (1985) pointed out that having a front width  $\delta w \sim H$ , although it does not affect much the Keplerian character of the flow, could lead to a Rayleigh-unstable situation in the disc. A comparison between the criterion derived by Lin et al. (1985) and the structure of the narrow heating fronts found here suggests that this type of fronts may indeed experience the development of a Rayleigh instability. This could result in an enhanced radial transport (Lin et al. 1985) and an additional uncertainty in  $J$ .

The equations used in this study are only valid in the thin disc approximation, i.e. when radial pressure gradients can be neglected and both  $\Omega$  and  $d\Omega/dR$  are equal to the Keplerian values. The effects of deviations from Keplerianity and radial pressure gradients were shown, for instance, by Ludwig & Meyer (1998) using full hydrodynamical disc equations and by Kley & Lin (1996) in boundary layer computations. Although these effects become non-negligible in

narrow heating fronts, we do not expect our main results on the structure and properties of transition fronts to be affected if they were fully taken into account. This could be checked by taking the full equations, which is beyond the scope of the present paper.

Finally, we note that the use of a local  $\alpha$ -prescription in narrow transition regions ( $\delta w \sim H$ ) is also subject to caution because the approach of scale separation becomes much less rigorous on scales so close to the size of the “turbulent eddies”.

## 7 DISCUSSION

Our simulations show that transition fronts systematically experience a deceleration during their propagation in the disc, whatever their direction of propagation. Yet, the front widths increase with radius in all the cases. This shows that the speed of a front is not directly related to its width (see also a related claim by Vishniac & Wheeler 1996 for cooling fronts). A description according to which the width of a transition front, which defines the gradients and the fluxes in the front, also determines its speed thus appears oversimplified.

Our simulations reveal a qualitative agreement with one of the predictions of the theory of infinitely thin transition fronts (Meyer 1984, 1986; see also Papaloizou & Pringle 1985): we clearly observe that the speed of transition fronts is related to the proximity of  $\Sigma$  in the disc to the critical values  $\Sigma_{\min}$  (for cooling fronts) and  $\Sigma_{\max}$  (for heating fronts).

Although Ludwig et al. (1994) pointed out that this theory may not be applicable to relatively broad cooling fronts, it could provide an explanation for the rapid deceleration of cooling fronts: the values of  $\Sigma$  around the region where the cooling front appears are close to  $\Sigma_{\min}$ , so that the front speed is initially high; soon, however, the front enters regions with larger and larger values of  $\Sigma$  as compared to  $\Sigma_{\min}$  (quasi-Shakura-Sunyaev profile), which results in a gradual decrease of the speed; later, the front must wait for the inner hot disc to evolve on a viscous timescale, typically, before  $\Sigma$  approaches  $\Sigma_{\min}$  in the disc, which explains the small speeds in the asymptotic regime. On the contrary, the speed of a heating front is able to remain large during the propagation, possibly because the profile of  $\Sigma$  encountered in the disc is typically in between  $\Sigma_{\min}$  and  $\Sigma_{\max}$  (Cannizzo 1993b), i.e. not too far from  $\Sigma_{\max}$  everywhere in the disc. If this is true, the deceleration of heating fronts is due to the (necessary) proximity of  $\Sigma$  to  $\Sigma_{\max}$  close to the ignition radius but not elsewhere in the disc.

We have not considered the structure and properties of transition fronts close to  $R_{\text{out}}$  in this paper. Indeed, additional simulations show that in a small region close to the disc outer edge, transition fronts are affected in a complex way if  $R_{\text{out}}$  is allowed to vary with time. The behavior of the fronts in this region of the disc may also depend sensitively on the precise choice of the outer boundary condition and how mass is deposited in the disc.

**8 CONCLUSION**

In this paper, we have investigated the structure and properties of transition fronts in thin accretion discs with detailed numerical calculations.

We showed that heating fronts are very narrow and have complex structures. They propagate at a speed which depends on the profile of surface density in the disc, the radial transport term in the energy equation and the value of the viscosity parameter  $\alpha$ , but is typically of order a few  $\text{km s}^{-1}$ .

Cooling fronts are broader, have a simpler structure and have smaller speeds (of order a fraction of a  $\text{km s}^{-1}$ ) than heating fronts. We found that their width is not equal to  $\sqrt{HR}$ , but is rather  $\propto H$ , the local disc scale height, as for heating fronts.

We confirmed that the structure of the inner hot disc is well described by a self-similar solution during the propagation of a cooling front. We proposed such a solution in which the surface density does not scale arbitrarily but with the value of the critical surface density  $\Sigma_{\text{min}}$ . The self-similarity of the disc appears responsible for the periodicity of the outburst cycles in the simulations.

Since all our models show a deceleration of transition fronts during their propagation in the disc, the observation of such a deceleration would constitute a nice confirmation that the thermal-viscous disc instability, as we understand it, is responsible for the large amplitude variability of discs around white dwarfs, neutron stars and black holes.

**ACKNOWLEDGMENTS**

We are grateful to Charles Gammie, Jean-Pierre Lasota, Ramesh Narayan, John Raymond and Ethan Vishniac for useful discussions. We also thank Guillaume Dubus and Eliot Quataert for comments on the manuscript. This work was supported in part by NASA grant NAG 5-2837. KM was supported by a SAO Predoctoral Fellowship and a French Higher Education Ministry grant. RS is supported by a PPARC Rolling Grant for theoretical astrophysics to the Astronomy Group at Leicester.

**REFERENCES**

Bath G.T., Pringle J.E., 1982, MNRAS, 199, 267  
 Bobinger A., Horne K., Mantel K.-H., Wolf S., 1997, A&A, 327, 1023  
 Cannizzo J.K., 1993a, ApJ, 419, 318  
 Cannizzo J.K., 1993b, in Wheeler J.C., ed., *Accretion Disks in Compact Stellar Systems*. World Scientific, Singapore, p. 6  
 Cannizzo J.K., 1994, ApJ, 435, 389  
 Cannizzo J.K., 1998a, ApJ, 494, 366  
 Cannizzo J.K., 1998b, in Howell S., Kuulkers E., Woodward C. eds., *Wild stars in the old west : proceedings of the 13th north american workshop on cataclysmic variables*. ASP Conference Series, vol. 137, p. 308  
 Cannizzo J.K., Chen W., Livio M., 1995, ApJ, 454, 880  
 Cannizzo J.K., Mattei J.A., 1992, ApJ, 401, 642  
 Chen W., Shrader C.R., Livio M., 1997, ApJ, 491, 312  
 Dubus G., Lasota J.-P., Hameury J.-M., Charles P., 1998, MNRAS, submitted  
 Faulkner J., Lin D.N.C., Papaloizou J., 1983, MNRAS, 205, 359  
 Frank J., King A., Raine D., 1992, *Accretion Power in Astrophysics*. Cambridge University Press, Cambridge

Hameury J.-M., Menou K., Dubus G., Lasota J.-P., Huré J.-M., 1998, MNRAS, 298, 1048  
 Ichikawa S., Osaki Y., 1992, PASJ, 44, 15  
 King A.R., Ritter H., 1998, MNRAS, 293, L42  
 Kley W., Lin D.N.C., 1996, 461, 933  
 Kuulkers E., Howell S.B., van Paradijs J., 1996, ApJ, 462, L87  
 Lasota J.-P., Hameury J.-M., 1998, in S. Holt & T. Kallman eds., *Accretion Processes in Astrophysics - Some Like it Hot*, in press, astro-ph/9712202  
 Lightman, A.P., 1974, ApJ, 194, 419  
 Lin D.N.C., Papaloizou J., Faulkner J., 1985, MNRAS, 212, 105  
 Ludwig K., Meyer F., 1998, A&A, 329, 559  
 Ludwig K., Meyer-Hofmeister E., Ritter H., 1994, A&A, 290, 473  
 Meyer F., 1984, A&A, 131, 303  
 Meyer F., 1986, MNRAS, 218, 7P  
 Mineshige S., Wheeler J.C., 1989, ApJ, 343, 241  
 Osaki Y., 1996, PASP, 108, 39  
 Papaloizou J.C.B., Pringle J.E., 1985, MNRAS, 217, 387  
 Pringle J.E., 1981, ARAA, 19, 137  
 Shahbaz T., Charles P.A., King A.R., 1998, MNRAS, in press, astro-ph/9807174  
 Shakura N. I., Sunyaev R.A., 1973, A&A, 24, 337  
 Smak J., 1984, Acta Astr., 34, 161  
 Vishniac E.T., 1997, ApJ, 482, 414  
 Vishniac E.T., Wheeler J.C., 1996, ApJ, 471, 921  
 van Paradijs J., Verbunt F., 1984, in S.E. Woosley, ed., *High Energy Transients in Astrophysics*, AIP Conf. Proc. 115, American Institute of Physics, New York, p.49  
 Warner B., 1995, *Cataclysmic Variable Stars*. Cambridge University Press, Cambridge